

The Affinity of GXXXG Motifs in Transmembrane Helix-Helix Interactions Is Modulated by Long-range Communication*

Received for publication, December 19, 2003
Published, JBC Papers in Press, February 5, 2004, DOI 10.1074/jbc.M313936200

Roman A. Melnyk^{‡§¶}, Sanguk Kim^{¶**}, A. Rachael Curran^{¶‡‡}, Donald M. Engelman^{§§¶¶},
James U. Bowie^{**¶¶}, and Charles M. Deber^{‡¶¶}

From the [‡]Division of Structural Biology and Biochemistry, Research Institute, Hospital for Sick Children, Toronto, Ontario M5G 1X8, Canada, [§]Department of Biochemistry, University of Toronto, Toronto, Ontario M5S 1A8, Canada, ^{**}Department of Chemistry and Biochemistry and UCLA-DOE Center for Genomics and Proteomics, UCLA, Los Angeles, California 90095-1570, and ^{§§}Department of Molecular Biophysics and Biochemistry, Yale University, New Haven, Connecticut 06520-8114

Sequence motifs are responsible for ensuring the proper assembly of transmembrane (TM) helices in the lipid bilayer. To understand the mechanism by which the affinity of a common TM-TM interactive motif is controlled at the sequence level, we compared two well characterized GXXXG motif-containing homodimers, those formed by human erythrocyte protein glycoporphin A (GpA, high-affinity dimer) and those formed by bacteriophage M13 major coat protein (MCP, low affinity dimer). In both constructs, the GXXXG motif is necessary for TM-TM association. Although the remaining interfacial residues (underlined) in GpA (LLXXGVXXGVXXT) differ from those in MCP (VVXXGAXXGIXXF), molecular modeling performed here indicated that GpA and MCP dimers possess the same overall fold. Thus, we could introduce GpA interfacial residues, alone and in combination, into the MCP sequence to help decrypt the determinants of dimer affinity. Using both *in vivo* TOXCAT assays and SDS-PAGE gel migration rates of synthetic peptides derived from TM regions of the proteins, we found that the most distal interfacial sites, 12 residues apart (and ~18 Å in structural space), work in concert to control TM-TM affinity synergistically.

widespread, mode of association is mediated by the so-called GXXXG motif, which is known to act as a universal scaffold for the assembly of both TM helices (2–9) and soluble α -helices (10). The GXXXG motif, where two glycine residues are separated by any three amino acids on a helical framework, gives rise to a flat surface region on one face of the helix. This arrangement of Gly residues permits the close approach of interacting helices, whereupon extensive packing interactions take place between pairs of surrounding residues. It has been proposed that a portion of the interactive strength of GXXXG-mediated associations may originate from inter-helix hydrogen bonds between C α hydrogens and carbonyl oxygen atoms on the adjacent helix (11).

The glycoporphin A transmembrane (GpA-TM) segment is a well characterized transmembrane helix dimer that associates with high affinity, principally by using a central GXXXG motif (3, 12). The details of side chain-side chain packing for GpA are known in considerable detail, having been gleaned originally from extensive mutagenesis experiments (3), computer modeling (13, 14) and, subsequently, from a high-resolution structural analysis using nuclear magnetic resonance (NMR) for the GpA dimer in both detergent micelles (12) and lipid bilayers (15).

Despite the high occurrence of the GXXXG motif in transmembrane helices (7), GpA-TM is the only GXXXG peptide dimer with a structure determined to high resolution (11). Thus, it is not clear whether other membrane proteins containing this motif adopt a similar dimeric fold to GpA or have alternate structure. Moreover, it is not known how residues surrounding GXXXG motifs “tailor” the affinity of their helix-helix interactions for the required structural and functional purposes. For instance, the transmembrane helix of the major coat protein of the M13 bacteriophage (MCP-TM) contains a GXXXG motif (2) and has been shown to self-associate using both *in vitro* (2, 16–20) and *in vivo* (21) techniques. However, unlike the highly stable GpA-TM dimer, the affinity of MCP-TM helix-helix self-association is comparatively weak (22). Indeed, such low affinity seems to be a requirement for phage viability (18), thus raising the intriguing notion that the MCP homodimer may not be optimized for stability, but is instead designed to be in flux between the monomeric and dimeric states during the life cycle of the phage (20).

The GpA and MCP systems thus afford the opportunity to directly investigate the detailed mechanism by which the stability of a GXXXG-mediated interaction is either optimized (in the case of GpA) or not (in the case of MCP). In the present work, we initially establish, by using a method developed to model TM helix oligomers (23), that the primary sequence of

After their biosynthesis and subsequent integration into a membrane, many transmembrane (TM)¹ helices associate with other pre-formed helices to form functional membrane protein domains (1). Specificity for a given helix-helix interaction is achieved through the appropriate presentation of complementary side chains, which serve as recognition elements between associating helices. The most highly studied, and apparently

* This work was supported, in part, by National Institutes of Health Grants GM54160 (to D. M. E.) and GM063919 (to J. U. B.), and by Canadian Institutes of Health Research (CIHR) Grant FRN5810 (to C. M. D.). The costs of publication of this article were defrayed in part by the payment of page charges. This article must therefore be hereby marked “advertisement” in accordance with 18 U.S.C. Section 1734 solely to indicate this fact.

[¶] These authors contributed equally to this work.

^{¶¶} Recipient of a CIHR Doctoral Award.

^{‡‡} Funded by Grant 060016/Z/99/Z from The Wellcome Trust.

^{¶¶¶} To whom correspondence should be addressed. E-mail: deber@sickkids.ca, bowie@mbi.ucla.edu, or donald.engelman@yale.edu.

¹ The abbreviations used are: TM, transmembrane; GpA, glycoporphin A; MCP, M13 major coat protein; TOXCAT assay, transmembrane helix association coupled with the expression of chloramphenicol acetyltransferase; MCP-TM, M13 major coat protein transmembrane segment; GpA-TM, glycoporphin A transmembrane segment; RMS, root-mean-square; Fmoc, *N*-(9-fluorenyl)methoxycarbonyl; CAT, chloramphenicol acetyltransferase; RMSD, root-mean-square deviation; wt, wild type.

MCP is compatible with the dimers of the type formed by GpA. Then, through systematic replacement of the interfacial residues of MCP with those of GpA, individually or in combination, we assess the relative contributions of the interfacial sites in stabilizing TM helix-helix interactions, using both *in vitro* (TM peptides) and *in vivo* (TOXCAT) techniques. These combined approaches provide a model in which TM helix-helix interactive motifs are modulated through the propagation of long range cooperative interactions along a 12-residue segment of the oligomeric interface.

EXPERIMENTAL PROCEDURES

Computation of MCP Oligomerization—The structures of MCP-TM helix (amino acids 25–42, AWAMVVVIVGATIGIKLF) and mutants were built as uniform α -helices having a backbone torsion angle of $\phi = -65^\circ$ and $\psi = -40^\circ$ (24) using the Insight II Biopolymer package (Accelrys). We used the backbone-dependent rotamer library program, SCWRL (25), to choose the side chain rotamers. Structure prediction of MCP dimer was carried out as described (23). Briefly, the dimer optimization started with 200 pairs of helices placed in random orientations with respect to each other. Then, the packing interaction of each helix pair was optimized by using the MC minimization method. The internal backbone and side-chain positions were kept fixed during the minimization, but the relative positions of the helices were given all six degrees of freedom. The energy function used was a softened van der Waals potential without any electrostatic component. The simulations were stopped after a maximum of 100,000 MC steps or if 15,000 steps occurred without moving to a lower energy. All six orientation parameters were changed during a step; a step of the same magnitude and direction was repeated if the previous step resulted in lower energy. The step size in each parameter was randomly selected. The temperature was initially set at 500 K and decreased linearly to 0.1 K over the first 50,000 steps. In this manner, we generated a large collection of independently optimized structures. After the MC simulations, the dimer structures were filtered to remove structures incompatible with the dimer symmetry. Then, we clustered the remaining structures by $C\alpha$ root-mean-square (RMS) distances using NMRCLUSTER (26). Finally, the median model from the largest cluster was selected as our final predicted structure. This method follows the hypothesis that the correct structure is likely to reside in a broader energy well than the other incorrect structures (27) and was previously successful in predicting homo-symmetric TM helix bundle structures (23).

Peptide Synthesis—Peptides corresponding to MCP residues 21–48 (with three added N-terminal lysine residues) were synthesized with standard Fmoc chemistry on a PerSeptive Biosystems Pioneer™ peptide synthesizer. Synthesis employed the Pioneer standard (45 min) cycle. Addition of Fmoc-protected labels was done during synthesis using an extended cycle (60 min). The HATU/DIEA activating pair was used with a 4-fold excess amino acid. A low-load (0.18–0.22 mmol/g) PAL-PEG-PS resin was used to produce an amidated C terminus. Peptides were cleaved with a mixture of 88% trifluoroacetic acid, 5% phenol, 5% ultra-pure water, 2% triisopropylsilane. Cleaved peptides were precipitated with ice-cold diethyl ether. Centrifuged pellets were dried in a desiccator, redissolved in ultra-pure water, and lyophilized. Crude peptide powder was dissolved in water, and 10 mg of peptide were loaded onto a C4 preparative reverse-phase high-pressure liquid chromatography (HPLC) column. The major peak from a water/MeCN gradient was collected and lyophilized. Mass spectrometry was used to confirm the molecular weight of the purified peptide, and the micro-BCA assay was used to determine peptide concentration. Analytical HPLC chromatography was employed to confirm the purity of peptides as >95% pure.

Circular Dichroism Spectroscopy—Circular dichroism spectra were recorded using a Jasco J-720 circular dichroism spectropolarimeter. Purified peptide samples were dissolved in buffer containing 10 mM Tris, 10 mM NaCl, pH 7.2 with 20 mM SDS or 30 mM β -octylglucopyranoside. Spectra were obtained at peptide concentrations between 20 and 50 μ M. Measurements were made using a quartz cuvette with a path-length of 0.1 mm. Spectral scans were performed from 250–190 nm, with a step-resolution of 0.2 nm, a speed of 20 nm/min, and a bandwidth of 1.0 nm.

SDS-PAGE—Samples were subjected to SDS-polyacrylamide gel electrophoresis using 4–12% NuPage precast gels (Novex, San Diego, CA). Samples were boiled for 5 min prior to loading.

Fluorescence Spectroscopy—Fluorescence spectroscopy (steady-state) fluorescence spectra were recorded on a Photon Technology Interna-

tional C-60 fluorescence spectrometer. Samples were examined in a stoppered 2-mm \times 10-mm quartz cuvette (Hellma, Concord, ON, Canada). Emission spectra were collected from 300 to 450 nm ($\lambda_{\text{exc}} = 295$ nm), 0.1 s/nm, bandpass 2 nm for excitation and emission. Small unilamellar vesicles of *Escherichia coli* lipids were made using the following procedure. Peptide samples were frozen at -80°C and lyophilized in rimless 12-mm \times 75-mm glass Pyrex tubes. *E. coli* polar lipid extract from Avanti Polar Lipids (Alabaster, AL) in chloroform was then aliquoted into tubes containing dried peptide samples. Organic solvent was removed by using a dry nitrogen stream and further lyophilized overnight. Samples were hydrated using 500 μ l of buffer (50 mM Tris-HCl, 50 mM NaCl, pH 8) and vortexed periodically for 30 min. Small unilamellar vesicles were formed using bath sonication (30-s bursts) until solutions were clear (10 min).

TOXCAT Chimera Construction—MCP TOXCAT constructs consist of an N-terminal DNA-binding domain of ToxR, a transmembrane domain, and the periplasmic maltose-binding protein. Individual constructs were cloned by mutating the wild-type MCP construct (kindly provided by J. Dawson) using the QuikChange site-directed mutagenesis kit (Stratagene) protocol using oligonucleotides \sim 20 base pairs long. The mutation was located in the center of the oligonucleotide. Constructs were transformed into *E. coli* NT326 (Male⁻) cells. Whole-cell lysates were used to estimate expression levels of the constructs. Samples were run on SDS-PAGE, and then Western analysis was carried out using antibodies against MBP (NEB). Blots were developed using goat anti-rabbit alkaline phosphatase secondary antibody (Pierce). The presence of MBP in the periplasm was confirmed by growth on minimal maltose media.

CAT Assays—Cell-free extracts were made by pelleting 200 μ l of cells at an A_{600} of 0.6, resuspending in 500 μ l of 0.1 M Tris, pH 8.0, then lysing with 20 μ l of 100 mM EDTA, 100 mM dithiothreitol, and 50 mM Tris, pH 8.0, and one drop of toluene, at 30°C for 30 min. The cell-free extract was then diluted 1:80 before being used in the CAT assays. Briefly, samples were incubated at 37°C with tritiated chloramphenicol and *n*-butyryl coenzyme A. After 90 min, the reaction was halted by partitioning the [³H]chloramphenicol-butyl CoA complex into xylene. The organic phase was washed and quantified using the radiolabel. All measurements were performed four times. Errors shown are standard deviations on four measurements.

RESULTS

Structural Similarity of MCP and GpA Dimer Structures—We first investigated whether the MCP-TM can dimerize to form a structure similar to the known GpA-TM dimer (12, 15) or whether alternative structures might be preferred. Therefore, we applied an algorithm shown to be effective at modeling homo-oligomeric TM helix bundles when the number of subunits is known (23). Using this program, a single, strongly favored model for the packing of MCP-TM was generated (see “Experimental Procedures”). In this model, the glycyl residues from the GXXXG motif are juxtaposed in the dimer interface, thus facilitating close helix-helix approach. Detailed examination of the final structure of the MCP-TM dimer revealed a strong resemblance to that of the GpA-TM dimer, notwithstanding significant differences in side chain volume of the non-Gly interfacial residues (Fig. 1). Both models display a right-handed, helix-helix crossing angle of approximately -40° . The $C\alpha$ RMSD between this model of the MCP-TM and the GpA-TM obtained from solid-state NMR distance measurements is only 1.6 Å, and for GpA-TM from solution, the NMR measurement is 2.1 Å (RMSD between the structure from solid and solution NMR is 0.8 Å). Thus, the side chains on MCP-TM can be considered to be sterically compatible with the side chains in the GpA-TM dimer structure and *vice versa*.

Comparison of MCP Model and GpA Interfaces—If MCP-TM and GpA-TM dimers adopt similar structures, then the differences in their relative helix-helix affinity must be attributable to differences in interactions involving the non-Gly residues in the respective interfaces. Fig. 2 shows an alignment of MCP and GpA sequences, with the interfacial residues labeled *a* through *g*. It is apparent that both interfaces possess, in addition to the embedded GXXXG motif at the *c* and *e* positions, a

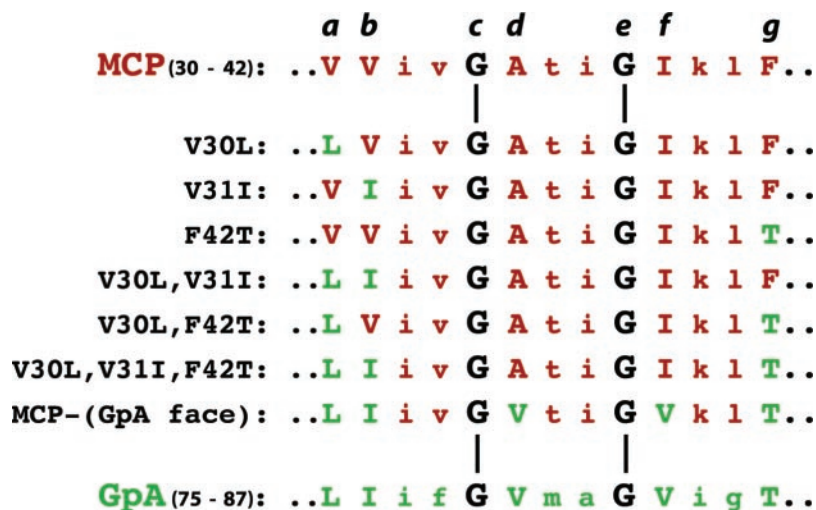


FIG. 3. Sequence alignment of constructs studied. Singly, doubly, and triply substituted MCP constructs are shown. For MCP-GpA, all of the dimer interfacial residues in MCP were changed simultaneously to those of GpA.

MCP sequence, this position would not be expected to contribute much to dimer affinity. Moreover, at position *b* (Ile⁷⁵ in GpA; Val³¹ in MCP), it was shown previously that both an I75V mutation in GpA and (in the opposite direction) a V31I mutation in MCP, had little or no effect on dimer stability for GpA and MCP, respectively (3).

The lack of significant affinity enhancement observed for single MCP mutants V30L and F42T was perhaps unexpected, especially given the dramatic effects the reverse changes have in the GpA background (see above). Thus, if interfacial residues contribute only individually to the stability of interacting helices, the results thus far would predict that no combination of these three mutants (V30L, V31I, F42T) should result in any additional stabilization of the MCP dimer. Yet, when the V30L and F42T mutants were combined to form the double MCP mutant V30L/F42T, a dramatic increase in stability was observed (Fig. 4C), resulting in a signal measuring ~70% of MCP-GpA. That the resulting affinity of this construct far exceeded the additive sum of the two mutants (~45% MCP-GpA) indicates that V30L and F42T work in tandem to stabilize the dimer in a synergistic fashion. The increase in affinity observed as one progresses from the triply substituted MCP (V30L/V31I/F42T), which is ~80% of the full MCP-GpA construct (V30L/V31I/A35V/I39V/F42T), thus points to a minor, but discernible, role for the *d* and *f* positions in contributing to dimer stability.

To investigate the mechanism underlying the stabilization imparted by the double mutant V30L/F42T, an additional mutant was generated in which the *g* position was substituted to Val, whereas the V30L substitution was retained (Fig 4D). For this double mutant (V30L/F42V), the size of the *g* side chain was retained, but the hydroxyl group was removed. The synergistic effect seen above for the V30L/F42T mutant was not observed for the V30L/F42V mutant (Fig. 4D), suggesting a discrete role of the hydroxyl group in stabilizing TM dimer affinity.

Oligomerization States of Synthetic Transmembrane Peptides—We next characterized the behavior of several of the GpA/MCP hybrid mutants in the context of synthetic TM peptides. Peptides afford the opportunity, not otherwise accessible in the TOXCAT constructs, to perform additional biophysical analyses on the isolated TM segments. MCP-TM peptides were designed to include the putative TM domain of MCP (residues 21–48), along with three non-native N-terminal Lys residues, which facilitate peptide synthesis, purification, and characterization (20). We reported previously that MCP-TM peptides designed in this manner were in equilibrium between the mo-

nomeric and dimeric states (20). The circular dichroism spectra of all of the present TM peptide constructs were superimposable in both SDS and in *n*-octyl-glucopyranoside and indicate about 70% helical content (Fig. 5A). The occurrence of a native Trp residue (Trp²⁶) in all MCP peptides allowed us to use fluorescence spectroscopy to further assess whether single- or multiple-mutations to the interface affected the stable insertion of peptides into detergents and phospholipid bilayers. As shown in Fig. 5B, Trp²⁶ fluorescence was blue-shifted (327–331 nm) and identical in both MCP wt and MCP-GpA, indicating comparable insertion properties in both detergent and phospholipid environments.

SDS-PAGE has proven to be a valuable tool to assess the association of TM segments for many different sequences (3, 29–40). Fig. 5C shows the migration behavior of the MCP peptide variants on SDS gels. We found that the migration of the TM peptides correlates well with the affinity measured by the TOXCAT assay. On the gels, a rapid equilibrium between monomeric and dimeric species is established, resulting in positioning of the dimer band as a function of both the degree of exchange and the relative population of the monomeric species. In particular, the low affinity MCP-wt peptide dimer migrates faster than the high-affinity MCP-GpA peptide. Migration rates of other mutants are largely consistent with affinities determined by TOXCAT assays.

DISCUSSION

The GXXXG motif provides a basic scaffold responsible for mediating TM helix-helix interactions. Indeed, early studies on GpA found that the central GXXXG portion was the most crucial part of the interaction motif, as judged by its hypersensitivity to mutation (3), and its ability to singularly mediate the assembly of otherwise monomeric sequences (41). The universality of this motif was demonstrated in a study wherein libraries were used to randomly select high-affinity TM sequences based on the two-in-two-out motif of GpA (6). Though biased to this right-handed crossing motif, it was found that 80% of the high-affinity isolates contained the GXXXG motif. The solution NMR structure of GpA further confirmed how the presence of the two Gly residues in the interface can facilitate the close approach of helices, thereby allowing extensive backbone-backbone and side chain-side chain interactions to occur (12). Analytical ultracentrifugation experiments have shown that mutation of any interfacial position along the GpA-TM to Ala is energetically costly (42). This is most significantly pronounced with Gly⁷⁹ and Gly⁸³, where the dimer is destabilized by 1.7 and 3.2 Kcal/mol, respectively. It has been suggested

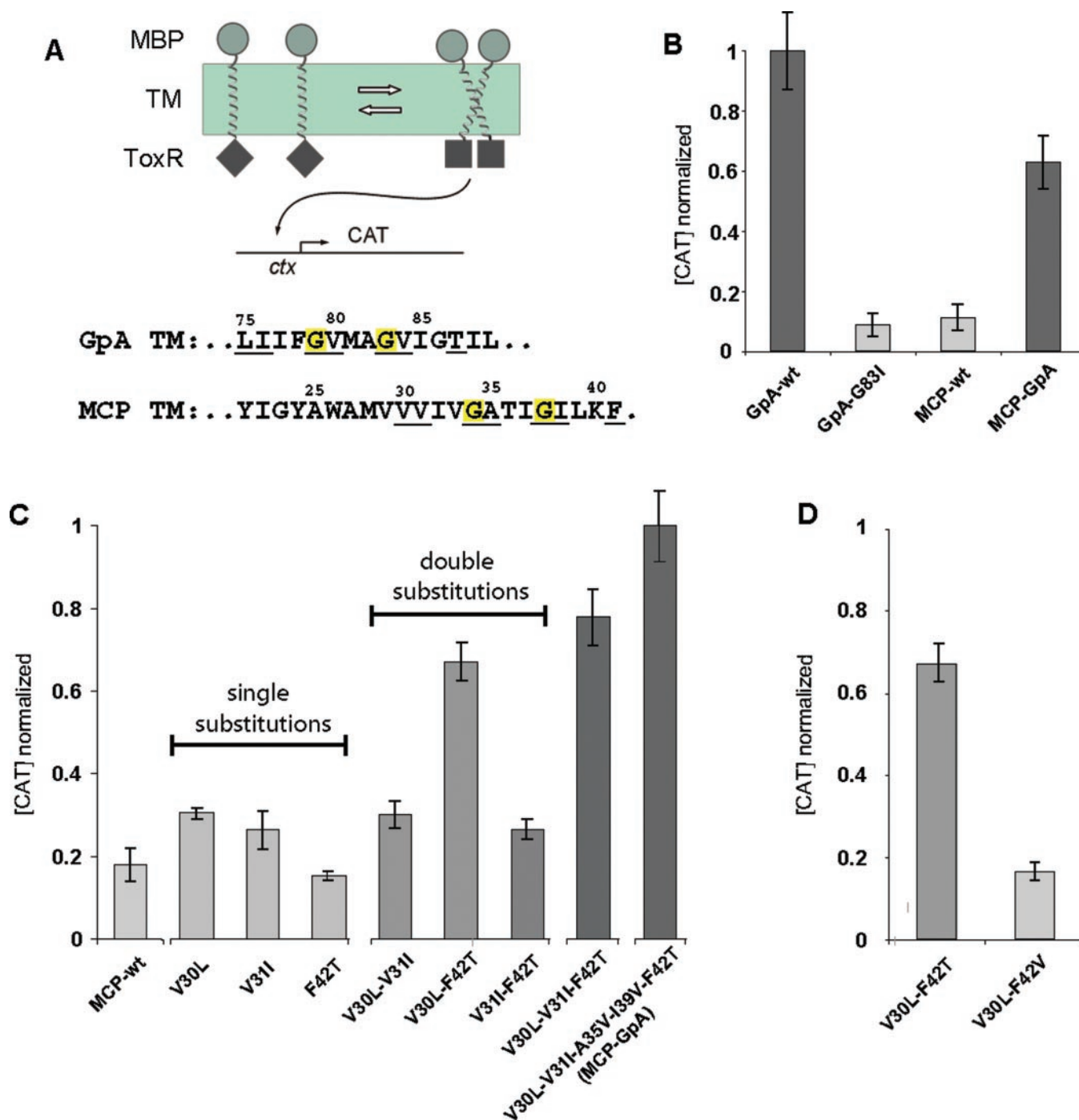


FIG. 4. TOXCAT assay to measure TM helix-helix affinity. **A**, TOXCAT assay to measure TM domain dimerization. The TM domain of interest is fused between the N-terminal ToxR transcriptional activator and the C-terminal, periplasmic maltose-binding protein (MBP). The sequences used for GpA-TM and MCP-TM are shown. The GXXXG motifs are not in equivalent positions relative to the ToxR and MBP domains. **B**, CAT levels normalized to GpA-wt. The dimer-disruptive mutant GpA-G83I is shown to illustrate the metastability of MCP-wt. Upon changing all of the interfacial residues in MCP to that of GpA (MCP-GpA), the CAT levels increased dramatically, albeit to levels that are lower than GpA-wt. MCP-GpA was used to normalize the remaining MCP constructs. **C**, CAT levels were normalized to MCP-GpA. Of the three singly substituted constructs, V30L shows a slight increase in association, whereas V31I and F42T did not enhance the dimerization relative to MCP-wt. Combining each of the single mutations into the three possible doubly substituted combinations illustrates the synergistic effect on dimer stability of combining V30L and F42T. The triply substituted construct shows a slight increase in dimer stability. Replacing the remaining two non-equivalent dimer interfacial residues in MCP to that of GpA results in an additional increase in the association of MCP. **D**, replacement of Phe⁴² in MCP to an isosteric residue (Val) in the double mutant V30L, F42V results in CAT levels that are comparable with MCP-wt, indicating the presence of an interhelical H-bond between Thr residues.

that the GXXXG motif may derive much of its interactive energy from the $C\alpha$ hydrogen of the Gly residues forming hydrogen bonds with the backbone carbonyls of the adjacent helix, which would have enhanced strength in the apolar lipid environment (11).

Here, we undertook a comparative analysis of two GXXXG-

containing TM sequences (GpA and MCP), both of which are involved in mediating homodimerization, but with very different affinities (22), and sought to understand how the non-Gly interfacial residues control the affinity of association. Other than their common GXXXG motif, there is no sequence identity between MCP and GpA at the five remaining interfacial sites:

FIG. 5. Helicity, insertion, and association of MCP-TM peptide constructs. The TM peptide constructs used had the prototypic sequence KKKYIGYAWAMVVVIVGATIGIKLFFKKFTSKAS. **A**, circular dichroism spectra of MCP-wt (\blacktriangle) and MCP-GpA (\circ) at 50 μ M in 1.5% β -octyl-glucopyranoside. **B**, tryptophan fluorescence emission maxima for MCP-wt and MCP-GpA in 1.5% β -octyl-glucopyranoside (black bars) and *E. coli* small unilamellar phospholipids vesicles (gray bars). **C**, SDS-PAGE of MCP variant peptides on 4–12% NuPage pre-cast gel. Arrows indicate the expected migration of fully monomeric (\bullet) or dimeric species ($\bullet\bullet$).

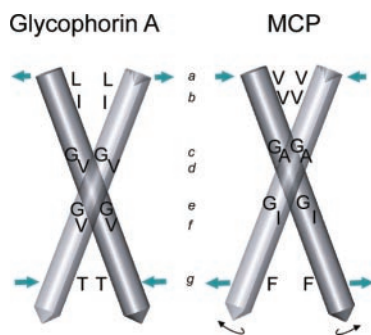
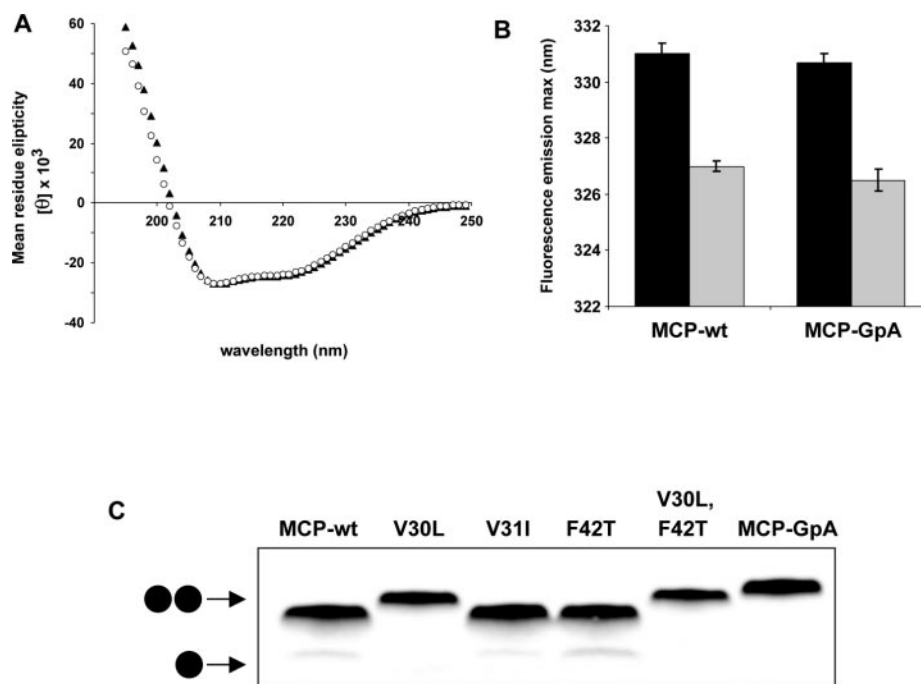


FIG. 6. Proposed mechanism of long-range coupling between the *a* and *g* positions in a TM helical dimer. The GpA and MCP-TM dimer models are shown as cylindrical representations, along with the inscription of interfacial residues from the *a* to *g* positions. The directional arrows illustrate the subtle difference in the dimerization interaction of two TM model helices induced by changing the side chain volumes in the packing interfaces.

a, *b*, *d*, *f*, and *g*. However, based on previous mutagenesis studies of GpA (2) that examined these positions in an extensive library, we reasoned that the differences at the *b*, *d*, and *f* positions would have only a marginal effect on affinity. As well, the observed hyper-variability observed at these sites in the high-affinity isolates obtained by Russ *et al.* (6) prompted us to focus principally on the *a* and *g* positions for the present study.

We found that it was necessary to convert both *a* and *g* positions of MCP to the corresponding GpA residues to impart the full stability effects, indicating that these residues, which are separated by 12 residues in the linear sequence and ~ 18 Å, as seen in the GpA-TM structure, act synergistically to stabilize the interface. As illustrated schematically in Fig. 6, we propose that the strong coupling between these two residues can be explained by the changes in structure induced by position *a*, which propagate along the helical axes to bring the residues in the *g* position into close proximity, allowing formation of an interhelical Thr-mediated hydrogen bond, either between two Thr hydroxyl substituents, or, as observed by Smith *et al.* (43), between the Thr hydroxyl and a backbone carbonyl group. The low affinity observed for the double mutant V30L/F42V allowed us to exclude both size and β -branching as the basis for the stability imparted by the residue at the

g position. The importance of the *a* position for facilitating this H-bond is underlined by the fact that the F42T construct alone, with Val at the *a* position, showed no increase in dimer affinity relative to MCP-wt. In effect, the *a* site acts as a molecular switch that controls whether an interaction (in this instance, an H-bond) can take place at the *g* position, and by extension, modulates the affinity of GXXXG-mediated interactions. Thus, three hallmark sequence features, present simultaneously, produce high TM-TM affinity: (i) a central GXXXG motif; (ii) a Leu residue at the *a* position; and (iii) either a Thr or Ser residue at the *g* position. The general sequence pattern LXXXGXXXGXXX(T/S) seems to represent a scaffold used by TM helices to ensure high-affinity interactions.

CONCLUSIONS

Recognition and assembly between TM helices are likely controlled by a small set of core sequence motifs. Of these, the GXXXG motif is one of the most over-represented motifs in TM segments (7). Using the comparative approach presented here, wherein a “weak” dimer (MCP) can be converted to a “strong” dimer (GpA) in a residue-dependent manner, we were able not only to delineate the contribution from each residue to dimer stability, but also to understand how side chains can communicate with each other over relatively long distances to synergistically control interaction affinity. Structurally, these results were validated by the gross similarity of the model structure of the MCP-TM dimer to the GpA-TM dimer. The 12-residue separation of the *a* and *g* positions along the TM helix indicates that long-range interactions play a direct role in the folding of TM domains in membrane proteins. Thus, although the GXXXG Gly residues are determinants of interfacial assembly, it is the surrounding interfacial residues that ultimately control and tune the affinity and dynamics of TM helix-helix interactions.

Acknowledgment—We thank Dr. Jessica Dawson for providing the MCP TOXCAT plasmid.

REFERENCES

1. Popot, J. L., and Engelman, D. M. (2000) *Annu. Rev. Biochem.* **69**, 881–922
2. Deber, C. M., Khan, A. R., Li, Z., Joansson, C., Glibowicka, M., and Wang, J. (1993) *Proc. Natl. Acad. Sci. U. S. A.* **90**, 11648–11652
3. Lemmon, M. A., Flanagan, J. M., Treutlein, H. R., Zhang, J., and Engelman, D. M. (1992) *Biochemistry* **31**, 12719–12725

4. Mendrola, J. M., Berger, M. B., King, M. C., and Lemmon, M. A. (2002) *J. Biol. Chem.* **277**, 4704–4712
5. Op De Beeck, A., Montserret, R., Duvet, S., Cocquerel, L., Cacan, R., Barberot, B., Le Maire, M., Penin, F., and Dubuisson, J. (2000) *J. Biol. Chem.* **275**, 31428–31437
6. Russ, W. P., and Engelman, D. M. (2000) *J. Mol. Biol.* **296**, 911–919
7. Senes, A., Gerstein, M., and Engelman, D. M. (2000) *J. Mol. Biol.* **296**, 921–936
8. Arselin, G., Giraud, M. F., Dautant, A., Vaillier, J., Brethes, D., Couлары-Salin, B., Schaeffer, J., and Velours, J. (2003) *Eur. J. Biochem.* **270**, 1875–1884
9. McClain, M. S., Iwamoto, H., Cao, P., Vinion-Dubiel, A. D., Li, Y., Szabo, G., Shao, Z., and Cover, T. L. (2003) *J. Biol. Chem.* **278**, 12101–12108
10. Kleiger, G., Grothe, R., Mallick, P., and Eisenberg, D. (2002) *Biochemistry* **41**, 5990–5997
11. Senes, A., Ubarretxena-Belandia, I., and Engelman, D. M. (2001) *Proc. Natl. Acad. Sci. U. S. A.* **98**, 9056–9061
12. MacKenzie, K. R., Prestegard, J. H., and Engelman, D. M. (1997) *Science* **276**, 131–133
13. Treutlein, H. R., Lemmon, M. A., Engelman, D. M., and Brunger, A. T. (1992) *Biochemistry* **31**, 12726–12732
14. Adams, P. D., Engelman, D. M., and Brunger, A. T. (1996) *Proteins* **26**, 257–261
15. Smith, S. O., Song, D., Shekar, S., Groesbeek, M., Ziliox, M., and Aimoto, S. (2001) *Biochemistry* **40**, 6553–6558
16. Makino, S., Woolford, Jr., J. L., Tanford, C., and Webster, R. E. (1975) *J. Biol. Chem.* **250**, 4327–4332
17. Cavalieri, S. J., Goldthwait, D. A., and Neet, K. E. (1976) *J. Mol. Biol.* **102**, 713–722
18. Henry, G. D., and Sykes, B. D. (1990) *J. Mol. Biol.* **212**, 11–14
19. Wang, C., and Deber, C. M. (2000) *J. Biol. Chem.* **275**, 16155–16159
20. Melnyk, R. A., Partridge, A. W., and Deber, C. M. (2002) *J. Mol. Biol.* **315**, 63–72
21. Haigh, N. G., and Webster, R. E. (1998) *J. Mol. Biol.* **279**, 19–29
22. Dawson, J. P., Melnyk, R. A., Deber, C. M., and Engelman, D. M. (2003) *J. Mol. Biol.* **331**, 255–262
23. Kim, S., Chamberlain, A. K., and Bowie, J. U. (2003) *J. Mol. Biol.* **329**, 831–840
24. Smith, L. J., Bolin, K. A., Schwalbe, H., MacArthur, M. W., Thornton, J. M., and Dobson, C. M. (1996) *J. Mol. Biol.* **255**, 494–506
25. Bower, M. J., Cohen, F. E., and Dunbrack, Jr., R. L. (1997) *J. Mol. Biol.* **267**, 1268–1282
26. Kelley, L. A., Gardner, S. P., and Sutcliffe, M. J. (1996) *Protein Eng.* **9**, 1063–1065
27. Shortle, D., Simons, K. T., and Baker, D. (1998) *Proc. Natl. Acad. Sci. U. S. A.* **95**, 11158–11162
28. Russ, W. P., and Engelman, D. M. (1999) *Proc. Natl. Acad. Sci. U. S. A.* **96**, 863–868
29. Arkin, I. T., Adams, P. D., MacKenzie, K. R., Lemmon, M. A., Brunger, A. T., and Engelman, D. M. (1994) *EMBO J.* **13**, 4757–4764
30. Simmerman, H. K., Kobayashi, Y. M., Autry, J. M., and Jones, L. R. (1996) *J. Biol. Chem.* **271**, 5941–5946
31. Mingarro, I., Whitley, P., Lemmon, M. A., and von Heijne, G. (1996) *Protein Sci.* **5**, 1339–1341
32. Mingarro, I., Elofsson, A., and von Heijne, G. (1997) *J. Mol. Biol.* **272**, 633–641
33. Fisher, L. E., Engelman, D. M., and Sturgis, J. N. (1999) *J. Mol. Biol.* **293**, 639–651
34. Bauer, C. M., Pinto, L. H., Cross, T. A., and Lamb, R. A. (1999) *Virology* **254**, 196–209
35. Lau, F. W., Nauli, S., Zhou, Y., and Bowie, J. U. (1999) *J. Mol. Biol.* **290**, 559–564
36. Laage, R., Rohde, J., Brosig, B., and Langosch, D. (2000) *J. Biol. Chem.* **275**, 17481–17487
37. Choma, C., Gratkowski, H., Lear, J. D., and DeGrado, W. F. (2000) *Nat. Struct. Biol.* **7**, 161–166
38. Karim, C. B., Marquardt, C. G., Stamm, J. D., Barany, G., and Thomas, D. D. (2000) *Biochemistry* **39**, 10892–10897
39. Nagy, J. K., Lau, F. W., Bowie, J. U., and Sanders, C. R. (2000) *Biochemistry* **39**, 4154–4164
40. Zhou, F. X., Merianos, H. J., Brunger, A. T., and Engelman, D. M. (2001) *Proc. Natl. Acad. Sci. U. S. A.* **98**, 2250–2255
41. Brosig, B., and Langosch, D. (1998) *Protein Sci.* **7**, 1052–1056
42. Fleming, K. G., and Engelman, D. M. (2001) *Proc. Natl. Acad. Sci. U. S. A.* **98**, 14340–14344
43. Smith, S. O., Eilers, M., Song, D., Crocker, E., Ying, W., Groesbeek, M., Metz, G., Ziliox, M., and Aimoto, S. (2002) *Biophys. J.* **82**, 2476–2486